Development of orientation in glassy polycarbonate at high strains

Nicole Heymans
Physique des Matériaux de Synthèse 194/8, Université Libre de Bruxelles, 1050 Brussels, Belgium
(Received 13 November 1986; revised 23 February 1987; accepted 3 March 1987)

Birefringence has been measured on yielded specimens of polycarbonate in simple tension in creep and stress relaxation. The pseudo-affine and random-chain affine models both fail to describe the experimental relationship between birefringence (or orientation) and strain. A new model assuming affine deformation of chain ends and non-random chains is presented, adequately describing the trends of experimental data.

(Keywords: molecular orientation; birefringence; glassy state; post yield; polycarbonate)

INTRODUCTION

It is general practice to describe development of orientation in partially crystalline polymers in the glassy state using Kratky's[1] pseudo-affine model (e.g. Spegt *et al.*[2], McBrierty and Ward[3] and Biangardi[4]). In this model, anisotropic units rotate as rigid rods in an affinely deforming isotropic matrix. The model has also been applied by Biangardi[4] and Mitchell *et al.*[5], among others, to orientation of amorphous polymers in the glassy state, although there is no justification for a two-phase model in this case. Kashiwagi *et al.*[6] have even applied the model to analysis of room temperature birefringence of poly(methyl methacrylate) (PMMA) deformed in the rubbery state. Orientation in the rubbery state is more usually described by Kuhn and Grün's[7] random-chain affine model (e.g. Purvis and Bower[8] and Cunningham *et al.*[9]); in this model, end-to-end vectors joining crosslinks (or 'entanglement points') deform affinely, and the chain is free to assume a random configuration between these points. Brown and Mitchell[10], Raha and Bowden[11] and Zanker and Bonart[12] attributed discrepancies to a strain-dependent entanglement density whereas Kahar *et al.*[13] attributed them to deviations from the statistical theory following an expression of the Mooney–Rivlin type.

Brown and Windle[14] have discussed the shortcomings both of the pseudo-affine model and of the random-chain affine model with variable entanglement density. They introduce a two-parameter model, separating strain into an 'extensional' and an 'orientational' component, successfully describing stress–strain and orientation–strain relationships in the rubbery state[15] (and Mitchell *et al.*[16]) and giving the general trends of glassy state behaviour[17].

In Erman and Flory's[18,19] description of crosslinked rubbers, diffuse entanglements are taken into account as restrictions on fluctuations of junctions, leading to non-affine deformation of end-to-end vectors. The theory describes birefringence in the rubbery state reasonably well; however, it has been shown by Gottlieb and Gaylord[20] that the theory breaks down completely (as do all existing theories of the rubbery state) when applied to stress–strain behaviour in swollen networks. Also, since the effect of entanglements is approximated by constraints on junctions (i.e. on chemical crosslinks) it does not appear possible to extrapolate the theory to thermoplastics.

It is interesting to note that all reasonably successful descriptions of the trends of deformation behaviour in polymers require at least two components of strain: orientational and extensional[14,16], phantom network with fluctuations[18], 'glide' mode and 'diffusional' mode (Lefebvre *et al.*[21]), uniformly affine and random chain affine (Picot *et al.*[22] and Maconnachie *et al.*[23]). This expresses the experimental fact that birefringence is not a unique function of strain, but also depends on time (at constant strain) or equivalently on strain history[13] as observed by Qayyum and White[24,25] and Hammack and Andrews[26]. Single component models, giving a one to one correspondence between orientation and strain[1,7] are clearly inadequate. Strictly speaking, two-component models only apply to the rubbery state; in the glassy state, description of the stress–strain behaviour has been shown by Bauwens[27] to require three components (Hookean spring, Eyring dashpot and rubbery-elastic spring).

The most convincing model to date of orientation behaviour in the glassy state has been given by Brown and Windle[14,17]. One drawback of their model, however, is that it ignores the fact that orienting units are joined into chains. The purpose of this paper is to propose an alternative model of orientation in the glassy state and to compare it with classical theories and with experimental data on birefringence in polycarbonate.

EXPERIMENTAL

Polycarbonate (PC) was chosen for this investigation, both because it is amorphous and because birefringence depends only on orientation of main chain segments, polarizability anisotropy being far greater for the phenyl ring than for the methyl side-groups.

Tensile specimens with flared ends and a gauge section $4 \times 0.8\ cm^2$ were cut from a commercially available sheet of polycarbonate (Makrolon, Bayer) 2 mm thick. The specimens were drawn in an Instron tensile tester at $0.5\ cm\ min^{-1}$ at room temperature until the neck had reached the flared ends. After unloading, the strain was

0032-3861/87/122009-09$03.00

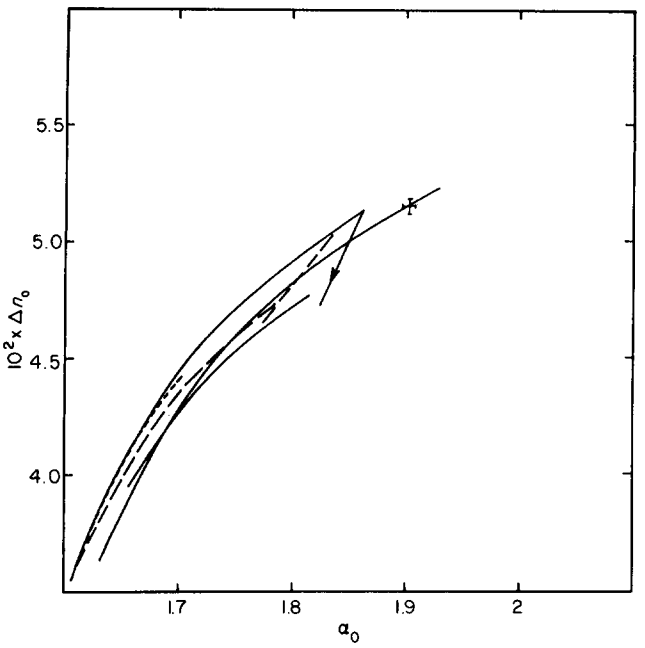

Figure 1 Residual birefringence against residual draw ratio at room temperature. Points omitted for clarity. ———, Creep; - - - - -, stress relaxation. Downward arrow indicates recovery. Error bars indicate uncertainty on variation of residual birefringence and draw ratio

determined from the change in cross-sectional area, and birefringence was measured in white light between crossed polars by comparison with a reference sample of known birefringence. The specimens were loaded in creep at nominal stresses (referred to the initial cross-section) ranging from 44 to 50 MPa at room temperature and from 32 to 44 MPa at 62°C. Strain was measured with a dial gauge and birefringence was measured between crossed polars in sodium light ($\lambda = 589.3$ nm) by counting fringes. A few samples were tested in stress relaxation, the total strain being stepped up regularly once relaxation had become negligible. Two short samples with flared ends and no gauge section were tested under the same conditions to obtain an estimate of the effect of creep of the tail pieces on strain measurements. It was found that the correction required to account for this effect was equivalent, within 2%, to assuming a gauge length of 50 mm instead of the nominal value, i.e. 40 mm. A few samples were tested below yield at room temperature, in creep and in tension at constant elongation rate.

For most samples a period of recovery of at least 24 h was allowed between sample preparation and testing. In order to determine whether variations in recovery time had any effect on subsequent behaviour, one sample was tested at room temperature within 30 min of preparation, and one was tested at 62°C without unloading.

RESULTS

Birefringence Δn was determined from fringe order f as:

$$\Delta n = \frac{\lambda f}{e_0(\alpha_0/\alpha)^{1/2}} \tag{1}$$

where λ is the wavelength of sodium light (589.3 nm), e_0 and α_0 are the thickness and draw ratio of the drawn sample prior to reloading and α is the current draw ratio. Birefringence at a given strain was found to increase with stress. This effect was assumed to be due to the purely elastic contribution of stress to birefringence and strain, which was found on unloading to be proportional to stress within experimental error. This contribution was evaluated from:

$$\Delta n_e = A\sigma \tag{2}$$

$$\Delta \alpha_e = \frac{\alpha\sigma}{E} \tag{3}$$

where σ is true stress, $A = 7.4 \times 10^{-5}$ MPa^{-1} and $E = 3400$ MPa at 20°C (6.5×10^{-5} MPa^{-1} and 3700 MPa respectively at 62°C). These are average values obtained from the immediate response on unloading. The slightly higher modulus at 62°C might simply reflect the lower stresses required at this temperature. These contributions were subtracted from all results obtained on samples under load, in order to convert them to an equivalent unstressed state. Corrected or residual values will be denoted by subscript 'o'. They are relatively insensitive to variations of A and E in creep; in stress relaxation experiments, the major cause of variation of birefringence is the change in stress, making results sensitive to any uncertainty in A and E, and consequently making them more difficult to interpret.

When Δn_0 is plotted against α_0 (*Figure 1*), curves obtained at different loads are extremely similar in shape, and differences between these plots do not depend on load. Remaining scatter appears to be traceable to differences in the initial state of the samples (i.e. after preparation but prior to testing). In *Figures 2* and *3*, results obtained on different samples have been arbitrarily shifted to superpose the shape of the final parts of the plots (i.e. long times and high strains). The shifts are not given, as they are extremely difficult to interpret: widely varying combinations of initial strain and birefringence can be obtained, depending on the strain at

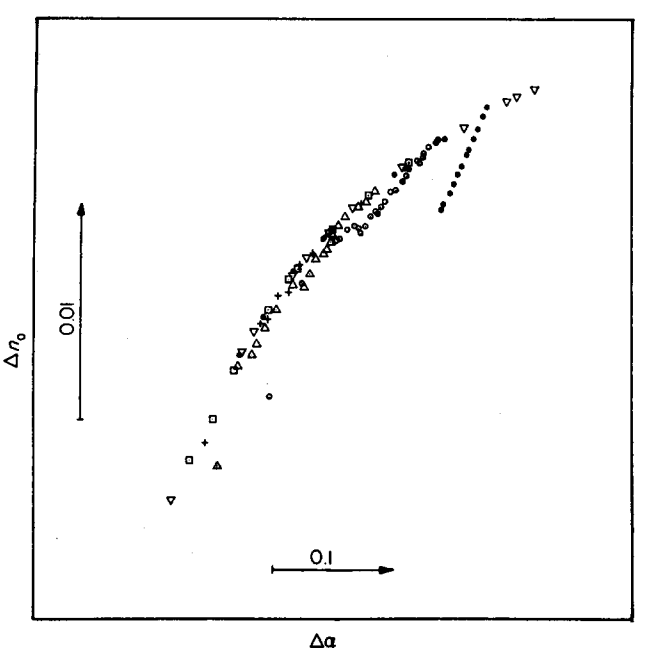

Figure 2 As *Figure 1* but curves shifted to superpose long-term portion. +, 52.5 MPa; ▽, 48.8 MPa; ●, 46.4 MPa and recovery after same; □, 44.2 MPa; ○, △, stress relaxation

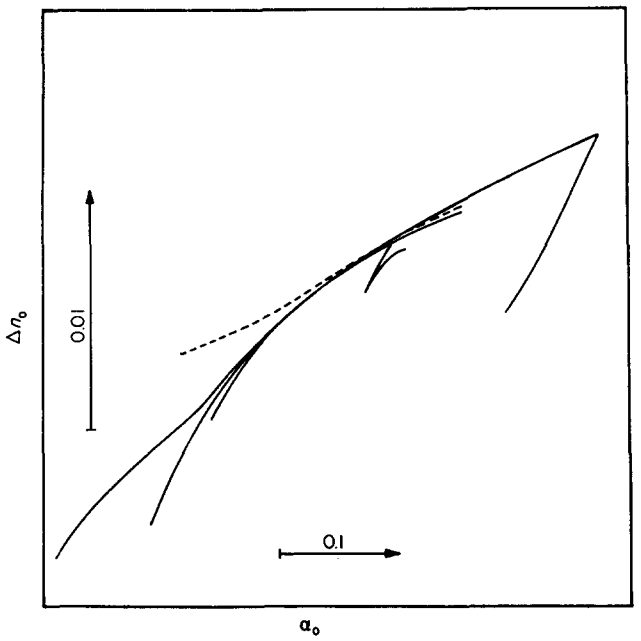

Figure 3 Residual birefringence against residual draw ratio at 62°C; ———, creep and interrupted creep after prestraining and recovery; ·····, sample tested in creep immediately after prestraining. Curves shifted to superpose long-term behaviour

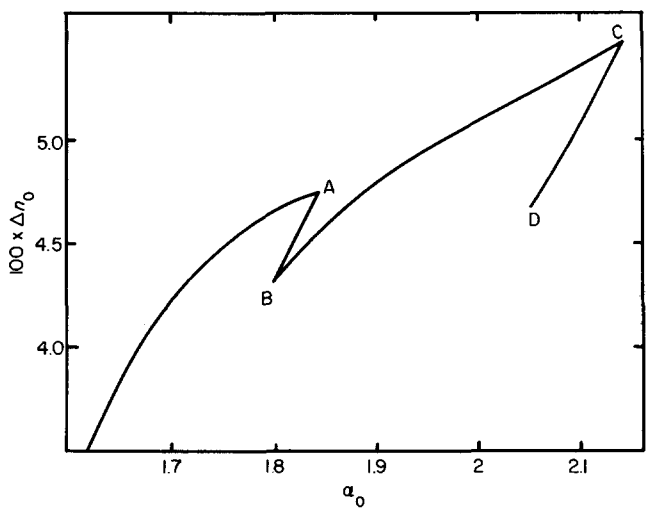

Figure 4 Residual birefringence against residual draw ratio during creep at 34 MPa (to A), recovery (AB), reloading at 41 MPa (BC) and recovery (CD) at 62°C

which drawing was interrupted, delay between drawing and creep and, for creep at 62°C, time allowed for temperature equilibration before creep.

In order to test the effect of sample preparation, two samples were tested at the same nominal stress (49 MPa) at room temperature, one after 30 min recovery and the other after 2 months recovery. It was found that although the initial linear portion of the plot was somewhat shorter for the first sample, there was very little difference between the subsequent behaviour of the two samples, and it was concluded at the time that behaviour at high strains was insensitive to sample preparation conditions. Another sample was clamped at fixed length after preparation (at room temperature) until it was loaded in creep at 62°C; in this case (broken line in *Figure 3*) the initial steep linear portion was suppressed completely. This is further evidenced by behaviour on unloading, recovery and reloading (*Figure 4*): during recovery, birefringence decreases linearly with strain, except perhaps at very long times (approaching *D*) where there appears to be a change in slope, although there are too few data points to be sure of this effect, which might reflect the tendency of the dial gauge to slip when the sample is not loaded; on reloading, birefringence first increases sharply with strain and then gradually approaches the extrapolated prior curve. These results suggest the coexistence of two components of orientation and strain: a 'fast' component associated with high orientation and low strain, and a 'slow' component associated with low orientation and high strain. This possibility will be developed more fully in the discussion.

Plots of strain against log time under load or after unloading are linear for as long as patience allows (*Figure 5*). As is the case for any quantity varying logarithmically with time, a characteristic time for creep or recovery can be defined at the intersection of the extrapolated linear part of the plot with a horizontal line at the level of the initial value; deviations from a straight line are, of course, observed at times shorter (or not much longer) than this characteristic time. At the time scale of our experiments, this only affects recovery. Both the fast and the slow component can be assumed to contribute to creep; on unloading, only the fast component recovers slowly, the slow component being ultra-slow. Linearity of the plot during creep, together with the small amplitude of recovery, lend support to the idea that the strain associated with the fast component is small. (At times sufficiently long for the slow component to recover, an increase in the slope is expected.)

The second order orientation function $\langle P_2 \rangle$ can be obtained from the measured birefringence Δn_0, if the maximum birefringence Δn_M corresponding to full chain extension is known, from:

$$\langle P_2 \rangle = \frac{\Delta n_0}{\Delta n_M} \tag{4}$$

By comparing birefringence with orientation functions obtained by WAXS, Biangardi[4] found $\Delta n_M = 0.236$ for

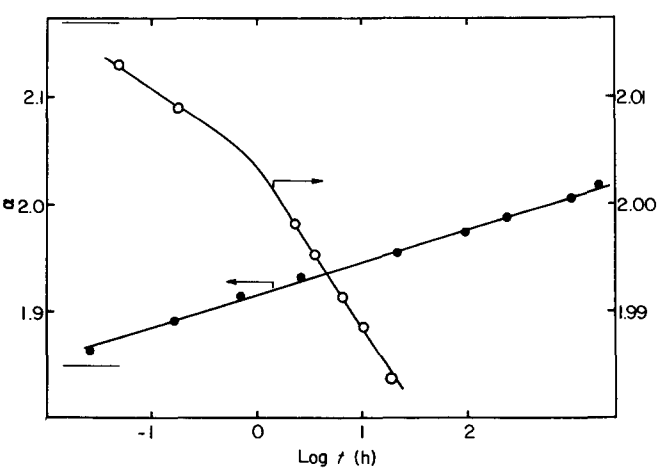

Figure 5 Variation of draw ratio during creep (●) (37 MPa) and recovery (○) at 62°C. Short horizontal lines indicate initial values of draw ratio

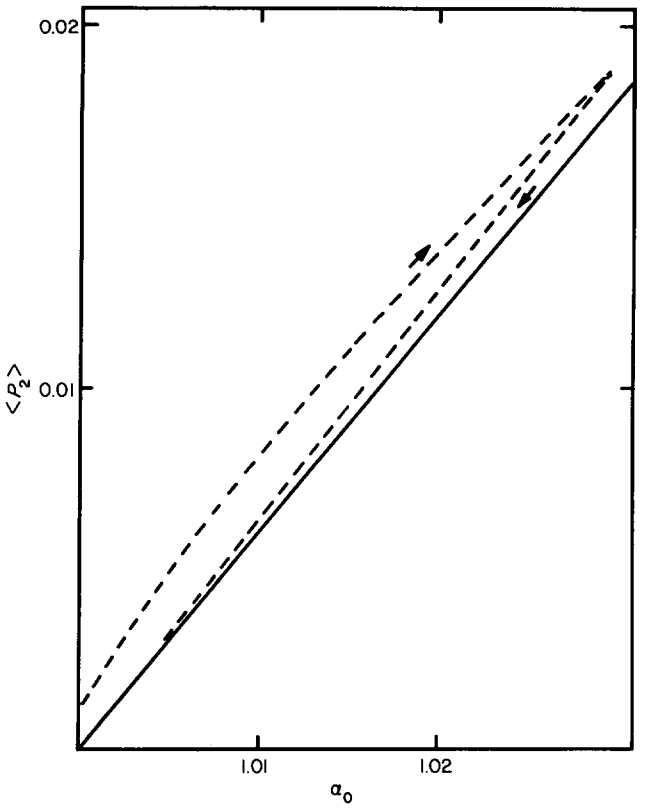

Figure 6 $\langle P_2 \rangle$ against draw ratio below yield; 20°C, 0.2 mm/min (up), 1 mm/min (down). ·····, Experimental, typical data. ———, Pseudo-affine theory

polycarbonate. Residual birefringence, converted to $\langle P_2 \rangle$, measured at low strains (i.e. below yield), is plotted against residual strain in *Figure 6*. No particular significance is given to the initial offset, which does not occur on the plot of total birefringence *versus* total strain. The offset might be caused by uncertainty in coefficients A and E used to determine the stress-dependent contribution; it does not affect the observation that the relationship between birefringence and strain is definitely non-linear, is not reversible and has a slope comparable to (and initially slightly larger than) that given by the pseudo-affine theory. All results, converted to $\langle P_2 \rangle$, are summarized in *Figure 7*, where they are compared with classical theories and with the model given in the next section.

THEORY

Introduction

The contribution of an anisotropic unit to the macroscopic anisotropy of a material property depends on the unit's anisotropy and on its orientation in the sample, defined by Euler angles θ, ϕ and ψ. (θ is the angle between the Z-axis of the unit and the z-axis of the reference frame; ϕ is the angle between the Z–z plane and the z–x reference plane and ψ is the angle between the X-axis of the unit and the Z–z plane.) The average macroscopic anisotropy will then depend on the orientation distribution function $h(\theta,\phi,\psi)$. If the unit is transverse isotropic or can rotate freely about its axis, $h(\theta,\phi,\psi)$ is independent of ψ. (In fact free rotation is not required; the requirement is simply that ψ must be uncorrelated with θ and ϕ.) If the sample is also transverse isotropic $h(\theta,\phi)$ becomes independent of ϕ. These conditions will be assumed to be fulfilled in what follows.

For computational purposes it is convenient to express $h(\theta)$ as an expansion in terms of a set of orthogonal functions; in the case of a large number of material properties (e.g. polarizability, sonic modulus, thermal expansivity, heat conduction, n.m.r. second moment, polarized fluorescence, Raman spectroscopy), the macroscopic anisotropy depends on products of low order powers of the direction cosines defining the orientation of structural units, and the spherical harmonics then form a particularly convenient set of orthogonal functions. In the event of transverse isotropy, both of the sample and the unit, these reduce to the Legendre polynomials of order l, $P_l(\cos\theta)$.

In the case of polymers it is often convenient to express segmental orientation as the convolution of the distribution $h_c(\cos\theta_c)$ of the orientations of chains (or portions thereof) with respect to the draw direction, with the distribution $h_s(\cos\theta_s)$ of segmental orientation with respect to the chain end-to-end vector. The segmental orientation distribution can then be expressed as:

$$h_s(\cos\theta_s) = \sum_l \frac{2l+1}{2} C_l P_l(\cos\theta_s) \tag{5}$$

where

$$C_l = \int_{-1}^{1} h_s(\cos\theta_s) P_l(\cos\theta_s) \mathrm{d}\cos\theta_s \tag{6}$$

and $P_l(\cos\theta_s)$ is the non-normalized Legendre

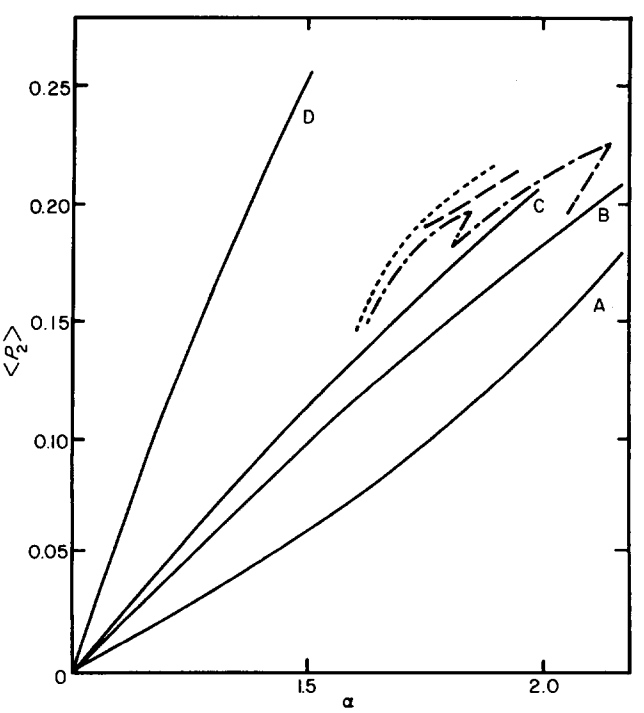

Figure 7 $\langle P_2 \rangle$ against draw ratio; full curves: theory. A, Rubbery affine, equation (11), 6 segments; B and C, equation (19), B: $C_{20}=0$, C: $C_{20}=0.1$; D, pseudo-affine, equation (12). Experimental results: ·····, 20°C; –·–·–, 62°C, strain history, see text; – – – –, 62°C, no recovery prior to creep

polynomial of order l, equal to:

$$P_l(\cos\theta_s)=\frac{1}{2^l l!}\cdot\frac{d^l}{d(\cos\theta_s)^l}(\cos^2\theta_s-1)^l \qquad (7)$$

(The normalized Legendre polynomial is given by the above expression, multiplied by $[(2l+1)/2]^{1/2}$. The non-normalized expression is more convenient in use because the orientation averages then vary between 0 for random orientation and 1 for perfect alignment.) C_l given by equation (6) will generally depend on θ_c through the effect of the end-to-end length of the chain on the orientation distribution; it will therefore be written $C_l(\cos\theta_c)$. The contribution of each chain to the macroscopic anisotropy will be proportional to $C_l(\cos\theta_c)$ and the orientation average is then given by:

$$\langle P_l\rangle=\int_{-1}^{1} h_c(\cos\theta_c)C_l(\cos\theta_c)P_l(\cos\theta_c)d\cos\theta_c \qquad (8)$$

Expressions for the orientation distribution of chains h_c and for the segmental orientation average C_l can then be obtained from an appropriate model for molecular deformation.

If affine deformation is assumed,

$$h_c(\cos\theta_c)=\frac{\delta^3}{2} \qquad (9)$$

where

$$\delta=\frac{\alpha}{[\alpha^3-\cos^2\theta_c(\alpha^3-1)]} \qquad (10)$$

is the extension ratio of a vector forming an angle θ_c with the draw direction in the deformed state, and α is the macroscopic draw ratio.

In the rubbery-elastic affine model, affine deformation is assumed for end-to-end vectors joining crosslinks (or entanglement points in a thermoplastic) and a random configuration is assumed for chains joining crosslinks. The orientation averages are then obtained using Treloar's closed form approximation to the inverse Langevin function; $\langle P_2\rangle$ has been given by Roe and Krigbaum[28]:

$$\langle P_2\rangle=\frac{1}{5\alpha_M^2}\left(\alpha^2-\frac{1}{\alpha}\right)+\frac{1}{25\alpha_M^4}\left\{\left(\alpha^2-\frac{1}{\alpha}\right)^2+\frac{7}{3\alpha}\left(\alpha^2-\frac{1}{\alpha}\right)\right\}+\frac{1}{35\alpha_M^6}\left\{\left(\alpha^2-\frac{1}{\alpha}\right)^3+\frac{18}{5\alpha}\left(\alpha^2-\frac{1}{\alpha}\right)^2+\frac{21}{5\alpha^2}\left(\alpha^2-\frac{1}{\alpha}\right)\right\} \qquad (11)$$

where α_M is the limiting network extension. $\langle P_4\rangle$ has been given by Nobbs and Bower[29], who also extended the theory beyond the affine limit.

In the pseudo-affine model, anisotropic units rotate within an affinely deforming matrix which makes no contribution to the macroscopic anisotropy. The orientation distribution of anisotropic units is given by equation (9); C_l is equal to 1 for all l. $\langle P_2\rangle$ is then equal to:

$$\langle P_2\rangle=\frac{1}{2}\left(\frac{2\alpha^3+1}{\alpha^3-1}-\frac{3\alpha^3\tan^{-1}(\alpha^3-1)^{1/2}}{(\alpha^3-1)^{3/2}}\right) \qquad (12)$$

The reader is referred to Brown and Windle[14] for the corresponding expression of $\langle P_4\rangle$.

Alternative model for glassy state deformation

The underlying hypotheses of both the affine and the pseudo-affine models are somewhat unrealistic when applied to thermoplastics in the glassy state. The pseudo-affine scheme is essentially a two-phase model, for which there is no physical justification in the amorphous state. The random chain assumption, on the other hand, is unlikely to be fulfilled in the glassy state as the large-scale motions required for randomization do not occur. An alternative model is given below.

Deformation is unlikely to be affine on the scale of a few monomers; however, it will always be possible to find a scale large enough for deformation to be assumed affine. The affine orientation distribution can therefore be assumed to apply to end-to-end vectors of chains, or of parts of chains (which shall be called subchains) of as yet undefined length.

Consider the subchain represented schematically in *Figure 8*. The orientation of a given anisotropic unit s with respect to the end-to-end vector r is defined by polar coordinates θ_s and ϕ_s. [ϕ_s is the azimuthal angle, i.e. the angle between the (s,r) and (z,r) planes.] Let us assume that the subchain deforms as though it were enclosed in an affinely deforming tube or shroud formed by neighbouring chains, i.e. if the length of the tube is proportional to δ, the cross-sectional area decreases like $1/\delta$.

As the cross-sectional area is proportional to $\langle\sin^2\theta_s\rangle$, this assumption is expressed by:

$$\langle\cos\theta_s\rangle=\delta\langle\cos\theta_s\rangle_0 \qquad (13)$$

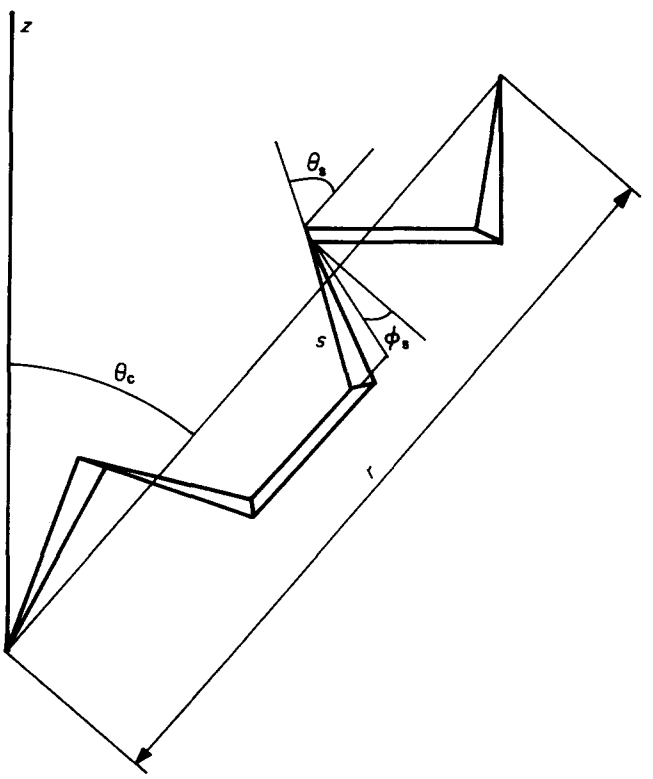

Figure 8 Schematic diagram of subchain defining coordinates used in the text

$$\langle \sin^2\theta_s \rangle = \frac{\langle \sin^2\theta_s \rangle_o}{\delta} \tag{14}$$

As

$$C_2 = 1 - \frac{3\langle \sin^2\theta_s \rangle}{2} \tag{15}$$

equation (14) can be rewritten:

$$1 - C_2 = \frac{1 - C_{2o}}{\delta} \tag{16}$$

where C_{2o} is the second-order segmental orientation average in the undeformed state. Introducing equation (16) and the affine distribution of end-to-end vectors, equation (9), into equation (8), the second-order orientation average is found as:

$$\langle P_2 \rangle = \int_{-1}^{1} \frac{\delta^3}{2}\left(1 - \frac{1 - C_{2o}}{\delta}\right)\frac{3\cos^2\theta_c - 1}{2} d\cos\theta_c \tag{17}$$

with δ given by equation (10).

Equation (17) can be integrated making use of the change of variable:

$$\cos\gamma = \left(\frac{\alpha^3 - 1}{\alpha^3}\right)^{1/2} \cos\theta_c \tag{18}$$

giving (putting $k = 1/\alpha^3$)

$$P_2 = \frac{2+k}{1-k} - \frac{3k^{1/2}}{2(1-k)^{3/2}}\cos^{-1}k^{1/2} - (1 - C_{2o})\frac{k^{1/3}}{4}\left\{\frac{2+k}{(1-k)^{3/2}}\ln\frac{1+(1-k)^{1/2}}{1-(1-k)^{1/2}} - \frac{6}{1-k}\right\} \tag{19}$$

Equation (19) can only describe orientation behaviour at draw ratios low enough for equation (14) to be valid; equation (14) can be rearranged as:

$$\langle \cos^2\theta_s \rangle = 1 - \frac{1}{\delta} + \frac{\langle \cos^2\theta_s \rangle_o}{\delta} \tag{20}$$

From equation (13)

$$\langle \cos\theta_s \rangle^2 = \delta^2 \langle \cos\theta_s \rangle_o^2 \tag{21}$$

The requirement that, for any real orientation distribution,

$$\langle \cos^2\theta_s \rangle \geq \langle \cos\theta_s \rangle^2 \tag{22}$$

can be written

$$\delta(1 - \delta^2\langle \cos\theta_{so} \rangle^2) \geq 1 - \langle \cos^2\theta_s \rangle_o \tag{23}$$

or, defining the maximum extension α_M as the extension corresponding to full segmental alignment,

$$\delta\left(1 - \frac{\delta^2}{\alpha_M^2}\right) \geq 1 - \langle \cos^2\theta_s \rangle_o \tag{24}$$

For $\alpha_M^2 = 6$ and $\langle \cos^2\theta_{so} \rangle = 0.4$ the maximum admissible value for δ is 2.06. It is worthwhile noting that in the limiting case $C_{2o} = 1$, equation (19) reduces to the pseudo-affine relation (equation 12), but that the theory is then invalid for all values of α.

An additional assumption is required to obtain higher order orientation averages. The fourth order Legendre polynomial can be written:

$$P_4 = \frac{35\sin^4\theta - 40\sin^2\theta + 8}{8} \tag{25}$$

The segmental orientation average with respect to the subchain end-to-end vector is:

$$C_4 = \frac{35\langle \sin^4\theta_s \rangle - 40\langle \sin^2\theta_s \rangle + 8}{8} \tag{26}$$

It is not unreasonable to assume that the standard deviation of the distribution of values of $\sin^2\theta_s$ decreases in proportion to the mean value as deformation proceeds; then

$$\langle \sin^4\theta_s \rangle = \frac{\langle \sin^4\theta_{so} \rangle}{\delta^2} \tag{27}$$

Introducing equations (27) and (14) into equation (26),

$$C_4 = 1 - \frac{1 - C_{4o}}{\delta^2} - \frac{10}{3}\frac{\delta - 1}{\delta^2}(1 - C_{2o}) \tag{28}$$

Finally, on introducing equations (28), (25) and (10) into equation (8) and integrating as for $\langle P_2 \rangle$, the fourth-order orientation average is found as (putting $k = 1/\alpha^3$):

$$\begin{aligned} P_4 = \frac{1}{8}\Bigg\{ & \frac{35(2+k)}{2(1-k)^2} - \frac{30}{1-k} \\ & + 3 - \left(\frac{105}{2(1-k)^2} - \frac{30}{1-k}\right)\frac{k^{1/2}}{(1-k)^{1/2}}\cos^{-1}k^{1/2}\Bigg\} \\ & - \frac{1 - C_{4o}}{8}\Bigg\{\frac{k^{2/3}}{1-k}\left(15 - \frac{35(5-2k)}{8(1-k)}\right) \\ & + \frac{k^{1/6}}{(1-k)^{1/2}}\cos^{-1}k^{1/2}\left(\frac{105}{8(1-k)^2} - \frac{15}{1-k} + 3\right)\Bigg\} \\ & + \frac{5(1 - C_{2o})}{12}\Bigg\{\frac{k^{2/3}}{1-k}\left(15 - \frac{35(5-2k)}{8(1-k)}\right) + \frac{k^{1/3}}{1-k}\left(\frac{35(4-k)}{3(1-k)} - 30\right) \\ & - \frac{k^{1/3}}{2(1-k)^{1/2}}\left(\frac{35}{(1-k)^2} - \frac{30}{1-k} + 3\right)\ln\frac{1+(1-k)^{1/2}}{1-(1-k)^{1/2}} \\ & + \frac{k^{1/6}\cos^{-1}k^{1/2}}{(1-k)^{1/2}}\left(\frac{105}{8(1-k)^{1/2}} - \frac{15}{1-k} + 3\right)\Bigg\} \end{aligned} \tag{29}$$

No attempt was made to find higher order orientation averages.

To be complete, values should be assigned to the parameters C_{2o} and C_{4o}. It may be assumed that when an unstrained polymer is cooled from the rubbery to the

glassy state, the rubbery state configuration is maintained. If affine deformation applies to an entanglement length of n statistical segments, the limiting extension will be $n^{1/2}$ and conversely the fractional extension of an entanglement length in the unstrained state is $n^{-1/2}$. (The justification for taking an entanglement length as a subchain is that an entanglement length appears to be the length of polymer chain which is effectively confined to a 'tube' or, equivalently, the shortest length at which motion of one end of the subchain is independent of constraints on the other end. This picture leads to a description of the entangled state which is supported by a wide variety of experimental data[30].) Using Treloar's approximation to the Langevin function, the second and fourth order orientation averages for a random chain at a fractional extension t can be written[29]:

$$C_2 = 0.6t^2 + 0.2t^4(1+t^2) \tag{30}$$

$$C_4 = \{-5t^2 + 94t^4 - 151t^6 + 7(16t^8 + 9t^{10} + 12t^{12} + 3t^{14} + t^{16})\}/225 \tag{31}$$

For an entanglement length of 6 statistical segments, corresponding to a maximum extension ratio of 2.45, $t_o = 1/2.45$, giving $C_{20} = 0.106$ and $C_{40} = 5.22 \times 10^{-3}$.

DISCUSSION

Birefringence and second-order orientation functions

Experimental results are compared with the pseudo-affine and rubbery-elastic affine predictions and with equation (19) in *Figures 6* and *7*.

There is, of course, some uncertainty about the absolute 'experimental' value of $\langle P_2 \rangle$ obtained from equation (4), due to uncertainty about the maximum birefringence of PC, which was found by Biangardi[4] as $\Delta n_M = 0.236$. This value has been the object of some discussion in the literature. By comparing orientation averages derived from WAXS and from thermal conductivity anisotropy with birefringence data, Pietralla *et al.*[31] obtained the maximum birefringence of PC as 0.106. They argue that Biangardi's analysis, based on anisotropy of the main amorphous halo, attributed to nearest-neighbour interchain correlations, is incorrect because he did not take into account the $c/8$ shift between neighbouring chains. (In fact Biangardi assumes neighbouring chains to be uncorrelated in the z direction.) However, the orientation averages obtained by Pietralla *et al.* from WAXS data vary widely according to the interatomic distance at which they are determined, because the calculated variation of the intrachain orientation parameter with the interatomic distance does not reproduce the experimental variation, due to oversimplifications in the model. Logically, the most reliable values of $\langle P_2 \rangle$ should be those obtained from the strongest peak in the experimental $P_2(R)$ data. These are the lowest, and give an intrinsic birefringence of approximately 0.23. On the other hand, orientation parameters obtained from thermal conductivity anisotropy are systematically higher than those obtained from WAXS; this could be an indication that the orientating unit relevant for thermal conductivity is not the same as that relevant for WAXS; it could also indicate that the model giving $\langle P_2 \rangle$ values from the experimental anisotropy is inadequate. These values are evidently too high: for a sample drawn at room temperature, presumably to the natural draw ratio, i.e. 1.6, Pietralla *et al.* obtain $\langle P_2 \rangle = 0.5$ from heat conduction measurements, whereas the theoretical upper limit, presumably given by the pseudo-affine model, is 0.3 at this draw ratio.

It would appear then that the intrinsic birefringence obtained by Pietralla *et al.* is too low; Biangardi's value is claimed to agree with that calculated from bond polarizabilities[4], and is not far removed from the generally accepted value of approximately 0.25 for poly(ethylene terephthalate) (PET)[4,8], which has a similar structure. It also agrees with the value obtained from Pietralla's data[31] when using the most reliable estimate for $\langle P_2 \rangle$; 'experimental' values of $\langle P_2 \rangle$ are therefore obtained from equation (4) taking $\Delta n_M = 0.236$.

The pseudo-affine model clearly gives orientation functions which are far too high, except in the pre-yield elastic region where experimental values fall slightly above the pseudo-affine prediction (*Figure 6*). The rubbery affine model predicts values which are too low; it also predicts a positive curvature. It might be argued that the affine model, using the Langevin approximation, is unrealistic when the number of statistical segments per chain is as low as 6, but it has been shown[32] that more realistic models give results which are numerically very close to those obtained using the Langevin approximation, even for very short chains. (With 6 statistical segments per chain the limiting network extension is 2.45 in agreement with the maximum extensibility of 2.5 calculated by Donald and Kramer[33] from the entanglement molecular weight of PC.)

The predictions of equation (19) are in qualitative agreement with experimental results for reasonable values of C_{20}, although the experimental and theoretical curves cross each other unless C_{20} is assumed to vary with draw ratio, in which case the present theory would do no better than any other 'variable constant' theory.

The stumbling block of all three theories given above is that they all predict a unique relationship between orientation and strain, although it is clear from *Figure 4* that this is not supported by experiment. Any valid description of glassy state orientation requires at least two components, as suggested by Brown and Windle[17]. In their description of polymer orientation, an ellipsoidal unit can either reorient (orientational component) or be displaced (extensional component) under the effect of an applied stress. The orientational component of strain depends on the aspect ratio of the orientating unit, and the extensional component is assumed not to introduce any orientation. The fact that units are joined into chains in a real polymer is largely ignored, except for the limitation on the extensional component. Moreover, a unique relationship is predicted between the orientational component and true stress; since no orientation is associated with the extensional component this implies that orientation should depend only on true stress; this is certainly not borne out by experimental data. Although Brown and Windle's model is attractive, in that it yields a good deal of insight into orientational behaviour, it does not lend itself to a quantitative comparison with data, for the reasons outlined above.

In analysing experimental results obtained in this work, these were converted to an 'equivalent unstressed

Table 1 Coefficients appearing in equation (29) for fourth-order orientation functions

	α									
	1.2	1.4	1.6	1.8	2	2.4	2.8	3.2	3.6	4
100A	1.48	5.05	9.75	14.92	20.2	30.1	38.8	46.2	52.4	57.6
100B	0.275	0.887	1.62	2.35	3.03	4.17	5.01	5.60	6.00	6.28
100C	1.61	5.42	10.24	15.35	20.3	29.1	36.1	41.4	45.3	48.1

state'. This is clearly insufficient to separate orientation into two independent components, as the resulting residual birefringence still depends not only on strain, but also on strain history. The facts that the ratio of variation of birefringence to variation of strain is the same on unloading as during subsequent recovery, that the length of the steep initial part of the plot on reloading is related to previous recovery, disappearing altogether when the sample is not allowed to recover, and that similar levels of residual birefringence are obtained at long times on samples with very different previous strain histories, suggest the coexistence of two components of orientation: one (component A) related to a low draw ratio and a high ratio of orientation to strain, similar to pseudo-affine behaviour; the other (component B) related to a high draw ratio and relatively low orientation. Component A might be associated with local orientation of the pseudo-affine kind, and component B with molecular rearrangements on the scale of an entangled length: it therefore seems logical to associate some orientation with component B. As orientation decreases linearly with strain on unloading and during recovery, component B appears to be vanishingly slow at low stresses, and to be activated only at high stresses in the glassy state. The fact that orientation is slightly lower at 62°C than at room temperature could be taken as an indication that component A reaches saturation at a stress-dependent level.

A quantitative decomposition of experimental results into components A and B does not seem possible at the present stage: during recovery, component A decreases logarithmically, with no hint of any approach to equilibrium, so that its amplitude cannot be determined directly from experiment in the temperature range investigated. The limiting orientation at high strains, or equivalently the orientation observed on the sample which was not allowed to relax before loading in creep (broken line in *Figure 3*) follows a plot which is approximately parallel to the predictions of equation (19) for vanishing C_{2_0}. This is not incompatible with a low limiting extension, indicating a short entanglement length: as shown above, $C_{2_0} = 0.1$ for a sub-chain of only 6 statistical segments.

The model given above, expressed by equation (19), now appears as a description of component B only. Both the pseudo-affine and rubbery affine models offer an inadequate description of this component: the orientation predicted by the pseudo-affine model is too high, and no reasonable decomposition can give an experimental relationship between orientation and strain presenting an upward curvature, as predicted by the rubbery affine model: this would require component A to reach a maximum and thereafter decrease, and there is no reason to suspect such behaviour. The globally affine subchain described by equation (19), combined with a high-orientation, low strain component therefore appears to offer the best description to date of orientation behaviour in the glassy state. More work is required, nearer to the glass transition, in order to separate these components and investigate them more fully.

Fourth-order orientation functions

Although birefringence gives no information about higher-order orientation averages, equation (29) can be compared with predictions of classical theories and with experimental data found in the literature. Equation (29) can be expressed as:

$$\langle P_4 \rangle = A - B(1 - C_{4_0}) - C(1 - C_{2_0}) \tag{32}$$

where A, B and C depend only on strain and are given in *Table 1*.

Data is frequently presented as a plot of $\langle \cos^4\theta \rangle$ against $\langle \cos^2\theta \rangle$[4,34,35]. This is an apparently elegant representation because it reduces data scatter. Conversely, it is insensitive to small variations of $\langle P_4 \rangle$. This can be seen by using equation (7) to express $\langle \cos^4\theta \rangle$ as:

$$\langle \cos^4\theta \rangle = \frac{30\langle \cos^2\theta \rangle - 3}{35} + \frac{8\langle P_4 \rangle}{35} \tag{33}$$

$$= \frac{1}{5} + \frac{4\langle P_2 \rangle}{7} + \frac{8\langle P_4 \rangle}{35} \tag{34}$$

As $\langle P_4 \rangle$ is generally small and has a low prefactor in equation (33), $\langle \cos^4\theta \rangle$ is dominated by the isotropic term and by $\langle P_2 \rangle$ or equivalently $\langle \cos^2\theta \rangle$. The difference between the pseudo-affine value of $\langle \cos^4\theta \rangle$ and the value obtained putting $\langle P_4 \rangle = 0$ in equation (33) is less than 5% for $\langle \cos^2\theta \rangle < 0.5$. A more sensitive plot, particularly at low orientations, is obtained by plotting $\langle P_4 \rangle$ against $\langle P_2 \rangle$ (refs. 19 and 36) (although as pointed out by Nobbs *et al.*[36]. the pseudo-affine and rubbery affine models do not differ greatly in their predictions of the relationship between $\langle P_2 \rangle$ and $\langle P_4 \rangle$), the most discriminating plot being $\langle P_4 \rangle$ or $\langle P_2 \rangle$ against α(refs. 16 and 37). $\langle P_4 \rangle$ is generally very small[37], or even negative[16] for PMMA deformed in plane strain compression at room temperature, at low to moderate strains, although large values have been obtained on PET tapes spun to high draw ratios[36]. Experimental determinations of $\langle P_4 \rangle$ invariably exhibit considerable scatter. It is illustrative of the difficulties in determining $\langle P_4 \rangle$ that experimental values larger than 1 have been found[8].

An adequate model of deformation should be able to predict negative values of $\langle P_4 \rangle$ in some cases. As shown in *Figure 9*, both the pseudo-affine and the rubbery affine model give positive values of $\langle P_4 \rangle$ at all strains. (The

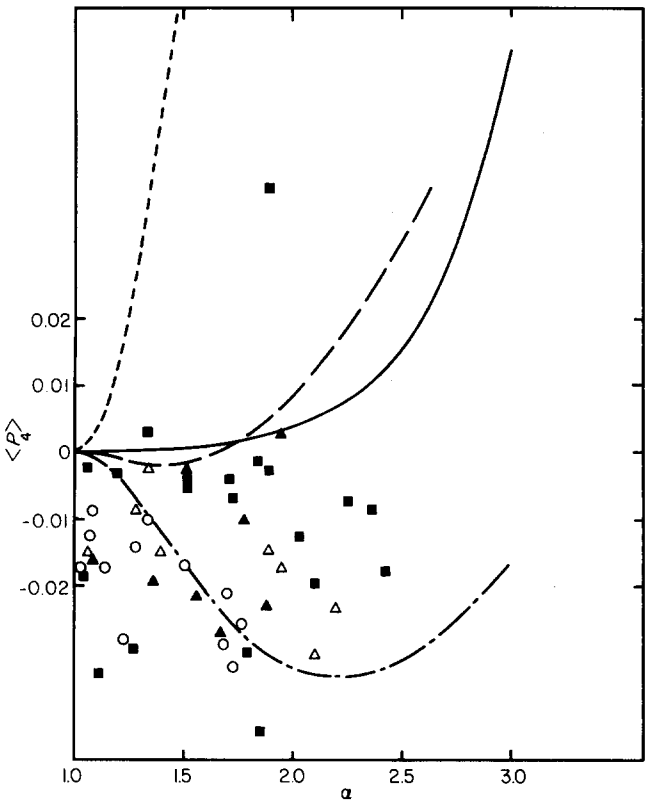

Figure 9 Fourth-order orientation function. Experimental points from Mitchell *et al.*[5] on PMMA: ○, 20°C; ▲, 40°C; △, 60°C; ■, 80°C. ····, Pseudo-affine theory (equation (29) with C_{20} and $C_{40}=1$); ———, rubbery affine with $n=10$ (from Nobbs and Bower[29]); equation (29), $C_{40}=0$; -·-·-, $C_{20}=0$; – – –, $C_{20}=0.2$

rubbery affine result is given for $n=10$ from Nobbs and Bower[29].) Brown and Windle's model[17] (not represented because numerical data were not available) gives negative values at low strains for all aspect ratios in the rubbery state, but $\langle P_4 \rangle$ becomes positive if rate effects are taken into account (i.e. in the glassy state). This would be rather the opposite to the effect suggested by comparing low temperature data (on PMMA[16]) with high temperature data (on PET[36]). Equation (29) is plotted in *Figure 9* for two values of C_{20} [which is effectively the sole parameter: the prefactor B of $(1-C_{40})$ in equations (29) or (32) is generally very small, and as C_{40} can also be assumed to be very small the product $B \cdot C_{40}$ can be omitted]. The model predicts negative values of $\langle P_4 \rangle$ at low strains, becoming positive at a draw ratio which varies with C_{20}. If C_{20} is sufficiently large, $\langle P_4 \rangle$ is positive at all draw ratios; the minimum value of C_{20} for this to occur is 0.28; if C_{20} is given by equation (30), this requires $t_0=0.63$, or an entanglement length of 2.5 statistical segments. This may seem ridiculously small, although as pointed out previously[30] polymers with very short entanglement lengths tend to crystallize, so that this behaviour is not unexpected for a crystallizable polymer such as PET. Moreover, in the discussion of $\langle P_4 \rangle$ so far, only one component of deformation has been considered (component B); if component A is also taken into account, and if the relationship between orientation and strain for this component is approximately pseudo-affine, the resulting value of $\langle P_4 \rangle$ will be less negative, and positive values will be obtained for a smaller strain, or for a lower initial segmental orientation (or equivalently a longer entanglement length).

CONCLUSION

There is no unique relationship between birefringence and strain in polycarbonate in the glassy state—birefringence depends on the entire strain history. An adequate description of orientation in the glassy state therefore requires at least two components of strain, both of which must be associated with a certain amount of orientation. A model incorporating these features has been given, in which one component of orientation is related to a globally affine model of deformation in which chain configurations are restricted by neighbouring chains; no interpretation has been attempted for the second component. This model is shown to give a good qualitative description of glassy state orientation in polycarbonate, and also of experimental values found in the literature of higher order orientation averages in other polymers.

ACKNOWLEDGEMENTS

I wish to thank Professor J. C. Bauwens for enthusiastic discussions in the course of this work.

REFERENCES

1 Kratky, O. *Kolloid Z.* 1933, **64**, 213
2 Spegt, P., Meurer, B., Hornick, C. and Weill, G. *J. Polym. Sci., Polym. Phys. Edn.* 1985, **23**, 315
3 McBrierty, J. and Ward, I. M. *Br. J. Appl. Phys. (J. Phys. D) Ser. 2* 1968, **1**, 1529
4 Biangardi, H. J. *Makromol. Chem.* 1982, **183**, 785
5 Mitchell, G. R., Pick, M. and Windle, A. H. *Polymer* 1983, **24** (*Commun.*), 16
6 Kashiwagi, M., Folkes, M. J. and Ward, I. M. *Polymer* 1971, **12**, 697
7 Kuhn, W. and Grün, F. *Kolloid Z.* 1942, **101**, 248
8 Purvis, J. and Bower, D. I. *J. Polym. Sci., Polym. Phys. Edn.* 1976, **14**, 1461
9 Cunningham, A., Ward, I. M., Willis, H. A. and Zichy, V. *Polymer* 1974, **15**, 749
10 Brown, D. J. and Mitchell, G. R. *Polym. Lett.* 1983, **21**, 341
11 Raha, S. and Bowden, P. B. *Polymer* 1972, **13**, 174
12 Zanker, H. and Bonart, R. *Colloid Polym. Sci.* 1981, **259**, 87
13 Kahar, N., Duckett, R. A. and Ward, I. M. *Polymer* 1978, **19**, 136
14 Brown, D. J. and Windle, A. H. *J. Mater. Sci.* 1984, **19**, 1997
15 *Idem ibid.* 1984, **19**, 2013
16 Mitchell, G. R., Brown, D. J. and Windle, A. H. *Polymer* 1985, **26**, 1755
17 Brown, D. J. and Windle, A. H. *J. Mater. Sci.* 1984, **19**, 2039
18 Erman, B. and Flory, P. J. *Macromolecules* 1983, **16**, 1601
19 *Idem ibid.* 1983, **16**, 1607
20 Gottlieb, M. and Gaylord, R. J. *Ibid.* 1984, **17**, 2024
21 Lefebvre, J. M., Escaig, B. and Picot, C. *Polymer* 1982, **23**, 1751
22 Picot, C., Duplessix, R., Decker, D., Benoit, H., Boué, F., Cotton, J. P., Daoud, M., Farnoux, B., Janninck, G., Neirlich, M., deVries, A. J. and Pincus, P. *Macromolecules* 1977, **10**, 436
23 Maconnachie, A., Allen, G. and Richards, R. W. *Polymer* 1981, **22**, 1157
24 Qayyum, M. M. and White, J. R. *Polymer* 1982, **23**, 129
25 *Idem J. Appl. Polym. Sci.* 1983, **28**, 2033
26 Hammack, T. J. and Andrews, R. D. *J. Appl. Phys.* 1965, **36**, 3574
27 Bauwens, J. C. *J. Mater. Sci.* 1978, **13**, 1443
28 Roe, R. J. and Krigbaum, W. R. *J. Appl. Phys.* 1964, **35**, 2215
29 Nobbs, J. H. and Bower, D. I. *Polymer* 1978, **19**, 1100
30 Heymans, N. *J. Mater. Sci.* 1986, **21**, 1919
31 Pietralla, M., Schubach, H. R., Dettenmaier, M. and Heise, B. *Prog. Colloid Polym. Sci.* 1985, **71**, 125
32 Heymans, N. *Polymer* 1986, **27**, 1177
33 Donald, A. M. and Kramer, E. J. *J. Polym. Sci., Polym. Phys. Edn.* 1982, **20**, 899
34 Purvis, J., Bower, D. I. and Ward, I. M. *Polymer* 1973, **14**, 398
35 Nobbs, J. H., Bower, D. I., Ward, I. M. and Patterson, D. *Ibid.* 1974, **15**, 287
36 Nobbs, J. H., Bower, D. I. and Ward, I. M. *Ibid.* 1976, **17**, 25
37 Mitchell, G. R. and Windle, A. H. *Ibid.* 1983, **24**, 285